DOI: http://dx.doi.org/10.15407/tpwj2018.09.03

# CHARACTERISTICS OF STRUCTURAL STRENGTH OF D16T ALLOY WELDED JOINTS, PRODUCED BY FRICTION STIR WELDING

**A.G. POKLYATSKY**[1], **Yu.V. GOLOVATYUK**[2], **T.M. LABUR**[1], **O.P. OSTASH**[2] and **S.I. MOTRUNICH**[1]
[1]E.O. Paton Electric Welding Institute of the NAS of Ukraine
11 Kazimir Malevich Str., 03150, Kyiv, Ukraine. E-mail: office@paton.kiev.ua
[2]G.V. Karpenko Physico-Mechanical Institute of the NAS of Ukraine
5 Nauchnaya Str., 79060, Lviv, Ukraine

A series of research was performed to study the characteristics of structural strength of butt joints of aluminium alloy D16T 2 mm thick, produced by friction stir welding. Features of weld formation and degree of metal softening in the zone of the produced permanent joint were analyzed. Mechanical testing of welded joint samples was performed at static and cyclic loading. Diagrams of fatigue crack growth rates in the base metal, heat-affected zone and thermomechanical impact zone, on the boundary of these zones and in the weld metal were plotted. It is shown that the characteristics of cyclic crack resistance of weld metal of these joints are more than two times higher than the respective values for base metal that is indicative of the good prospects for application of friction stir welding in fabrication of critical structures from D16T alloy. 19 Ref., 8 Figures.

***Keywords:*** *aluminium alloy D16T, friction stir welding, microstructure, cyclic crack resistance, structural strength*

Aluminium alloys of different alloying systems are widely applied in aerospace engineering [1, 2]. This is due to a combination of low metal content of aluminium alloys and quite high values of strength and crack resistance that together provide a reliable and long-term operation of metal structure assemblies [3]. Under the conditions of cyclic loading, the structural strength [4] is evaluated by complex parameter $[\sigma_t \Delta K_{th} K_{fc}]$, where $\sigma_t$ is the material ultimate strength, as well as the values of material cyclic crack resistance: $\Delta K_{th}$ is the fatigue threshold; $\Delta K_{fc}$ is the cyclic fracture toughness [5]. These parameters are particularly important at operation of structures by the fail-safe concept [6].

In fabrication of aerospace engineering components various methods of welding these aluminium alloys are used to produce permanent joints. Here, certain problems often arise due both to chemical composition of the aluminium alloys being welded, and to the welding process, which lead to lowering of welded joint structural strength. In particular, this is metal softening in the permanent joint zone [7], and formation of cast coarse-grained structure of welds [8], and appearance of characteristic defects in the form of pores, oxide film macroinclusions and hot solidification cracks [9–11]. Therefore, the available welding technologies are optimized, and new methods to produce permanent joints are developed, in order to improve the performance of aluminium alloy components.

The method of friction stir welding (FSW) is considered to be one of the most promising in fabrication of critical structures, including aerospace engineering. It was developed in 1991 at The Welding Institute as a method to produce joints in the solid phase [12]. FSW process has a characteristic difference from other pressure welding processes, due, mainly, to application of a special welding tool (Figure 1). Therefore, the main stages of permanent joint formation are directly related to this tool. Metal heating up to the plastic state, as well as prior cleaning of the surfaces of edges to be welded from oxide film, as a result of their friction with the shoulder working surface, take

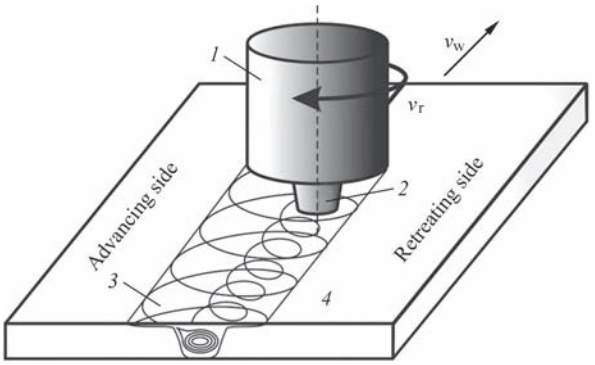


**Figure 1.** Schematic of FSW process: *1* — tool shoulder; *2* — tool pin; *3* — weld; *4* — welded blanks

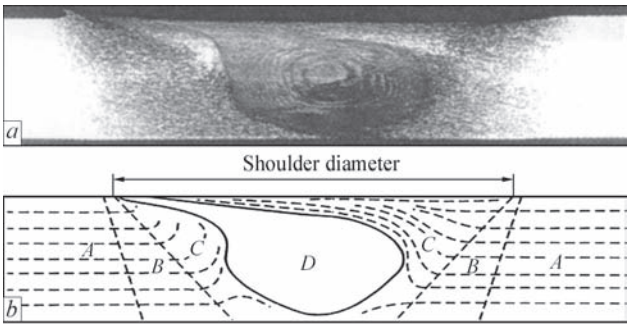


**Figure 2.** Transverse macrosection of the welded joint, produced by FSW (*a*) and respective schematic image of its characteristic zones

place under the tool shoulder. Owing to slight immersion of the tool into the metal being welded and its inclination relative to the vertical axis, the metal is in constant contact with the shoulder leading edge, forming a wave of plasticized metal owing welded. Mixing across the entire thickness occurs due to rotation of the tool pin. Metal heated up to the plastic state due to high adhesion of aluminium, is entrained by the pin side surface and is plastically deformed, moving after it. It results in intensive mass transfer of the metal being welded, at which the edges being welded are cleaned from oxide films and come into contact. Owing to intensive plastic deformation and heating, the metal goes into the plastic state, and its grains in the zone of direct impact of the tool are refined significantly that additionally promotes its viscoplastic flow. Under the shoulder rear edge, owing to tool inclination in the vertical plane, conditions are in place for additional compression of metal, moved into this zone by the pin side surface, that promotes running of relaxation processes (dynamic recrystallization, relaxation of welding stresses), as well as metal densification. Thus, physical contact at FSW is the result of degradation of the butt boundary under the impact of a special tool in the bulk limited by the tool working surfaces, substrate and the metal being welded proper.

Themomechanical conditions, at which permanent joints form in FSW result in a specific weld structure (Figure 2). Unlike welds of a cast structure, characteristic for fusion welding processes, they have fine

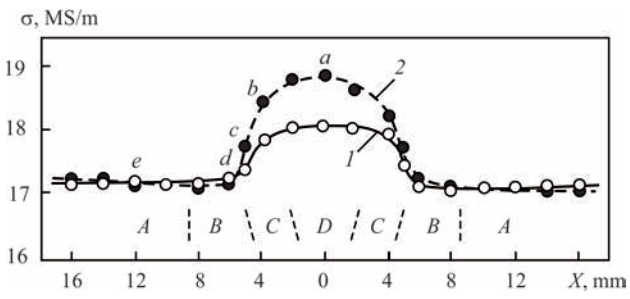


**Figure 3.** Change of specific electric conductivity on the sample face (*1*) and root (*2*) surfaces in the characteristic zones of FSW joint

deformed structure, with a clear-cut nugget *D* formed as a result of dynamic recrystallization, with up to 10 μm grain size. Bending, elongation and partial recrystallization of the grains proceed in the thermomechanical impact zone (TMIZ) *C*, adjacent to the nugget, as here the metal is subjected to heating and plastic deformation. Behind this area is the HAZ *B*, in which the metal remains undeformed and changes its structure only as a result of temperature rise. Next comes base metal zone *A*, where the metal does not undergo any changes [13, 14].

The objective of this work is evaluation of strength characteristics and cyclic crack resistance of welded joints of D16T alloy 2 mm thick, produced by FSW.

**Experimental procedure.** Investigations were conducted on butt joints of D16T alloy sheets (wt.%: 4.5 Cu; 1.7 Mg; 0.53 Mn; 0.19 Si; 0.21 Fe; 0.11 Zr; 0.06Ti; bal. — Al); welded along the rolling direction. Ultimate strength of this alloy sheets in the state after hardening and natural ageing $\sigma_t$ = 445 MPa, and relative elongation $\delta$ = 11 %. FSW process was performed in a laboratory unit developed at PWI. The rate of rotation of special welding tool [15] with a conical pin and 12 mm dia shoulder was 1420 rpm, and the speed of its linear displacement (welding speed) was 10 m/h.

Investigations were conducted in different zones of the welded joint (see Figure 2): in the weld central part (nugget), on the boundary of thermomechanical impact and heat-affected zones, in TMIZ and HAZ at 1 mm distance from this boundary, as well as in the base metal. These areas were selected in the characteristic points of change of local values of metal specific electric conductivity (Figure 3, points *a–f*), which is the physical characteristic of aluminium alloys, sensitive to the change of their structure and local stress-strain state, occurring during welding [3]. Values of specific electric conductivity were measured, using the eddy current method, with 1 mm step at alternating current frequency of 100 kHz that ensured the control depth up to 2 mm [16].

Metal hardness was measured on face surfaces of the produced welded joints. Degree of metal softening in the welding zone was assessed in ROCKWELL instrument at the load *P* = 600 N. Evaluation of structural features of welded joints was performed in MIM-8 optical electronic microscope. Ultimate strength of welded joints $\sigma_t^{w.j}$ and weld metal $\sigma_t^{w.m}$ was determined on standard samples with test portion width of 15 mm. Characteristics of cyclic crack resistance were determined on samples-strips 30 mm wide with side sharp (0.1 mm radius) U-shaped notch 2 mm deep along the axis of the studied zone of the welded joint, in keeping with the procedure, accepted

by ASTM International [17]. Obtained experimental data were the basis to plot the diagrams of fatigue macrocrack growth rates — $da/dN - \Delta K$ dependencies at the frequency of 10–12 Hz and coefficient of asymmetry $R = 0.1$ of the loading cycle in atmosphere at room (20 °C) temperature. Crack length was measured by cathetometer KM-6 at 25-fold magnification with 0.02 mm error. Obtained results were described by the respective analytical dependencies:

$$da/dN = C_1(\Delta K - \Delta K_{th})^{n1}, \text{ if } 10^{-10} \le da/dN \le 10^{-8}, \text{ m/cycle;} \quad (1)$$

$$da/dN = C_2(\Delta K)^{n2}, \text{ if } 10^{-8} \le da/dN \le 10^{-5}, \text{ m/cycle,} \quad (2)$$

where $da$ is the increment of crack length between the two successive measurements; $dN$ is the number of loading cycles between two successive measurements; $n1$, $n2$ is the exponent determined in keeping with the procedure of [17].

Diagrams of fatigue macrocrack growth rates were shown by lines, corresponding to these dependencies. The parameters selected as cyclic crack resistance characteristics were fatigue threshold $\Delta K_{th} = \Delta K_{10}^{-10}$ and cyclic fracture toughness $\Delta K_{fc} = \Delta K_{10}^{-5}$ the ranges of stress intensity factors $\Delta K$ at the crack growth rate $da/dN = 10^{-10}$, m/cycle and $10^{-5}$, m/cycle, respectively. Microfractographic features of fatigue fracture of samples were studied in a scanning electron microscope ZeisEVO-40XPV.

**Investigation results and discussion.** Performed investigations showed that the weld shape and dimensions in friction stir welding differ favourably from the weld produced by nonconsumable electrode argon-arc welding (GTAW) due to weld formation on a backing without the forming groove and producing a permanent joint without filler wire application (Figure 4). Absence of reinforcement or complete penetration in it allows avoiding high levels of stress concentration in the points of weld to base metal transition, adversely affecting the performance and life characteristics of welded joints.

In addition, permanent joint formation in the solid phase without base material melting prevents appearance of characteristic defects arising in fusion welding of aluminium alloys. So, absence of molten metal, in which hydrogen solubility increases markedly, allows avoiding additional saturation of the welding zone by it, because of migration of this gas from the adjacent metal layers and pore formation. Now, deformation and intensive stirring of plasticized metal over the entire thickness of the edges during welding, promoted fragmentation of oxide films present in them. Absence of molten metal in the zone of permanent joint formation allows avoiding its oxidation during welding. Therefore, welds, obtained by friction stir welding

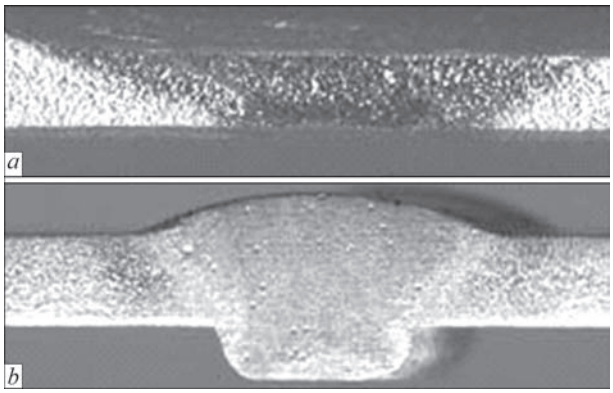


**Figure 4.** Transverse sections of welds of 2 mm alloy D16T produced by friction stir (*a*) and TIG welding (*b*)

have no defects in the form of oxide film macroinclusions, appearing in GTAW. The most hazardous and inadmissible defects for critical structures are hot cracks, forming during molten metal solidification in the point of accumulation of low-melting eutectic inclusions. As in friction stir welding the weld forms in the solid phase, and processes of metal melting and solidification are absent, formation of such defects can be completely avoided.

Features of weld formation in friction stir welding also have a favourable effect on the degree of metal softening in the zone of permanent joint formation. So, metal hardness measurements in the zone of permanent joint formation showed that in friction stir welding of D16T alloy, weld metal hardness practically is on the level of base metal (Figure 5). In the thermomechanical impact zone metal hardness gradually decreases at greater distance from the weld, reaching minimum value (*HRB* 97–98) at the boundary of the thermomechanical impact and heat-affected zones that corresponds to the point of lowering of specific electric conductivity (see Figure 3). Therefore, at uniaxial static tension samples of friction-stir welded joints have a high (425 MPa) yield limit and fail near the boundary of abutment of the thermomechanical impact zone to the heat-affected zone, where the metal hardness is minimum.

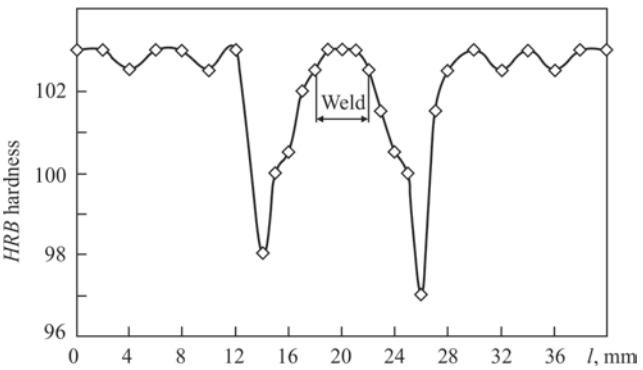


**Figure 5.** Hardness distribution in welded joints of D16T alloy 2 mm thick, produced by FSW

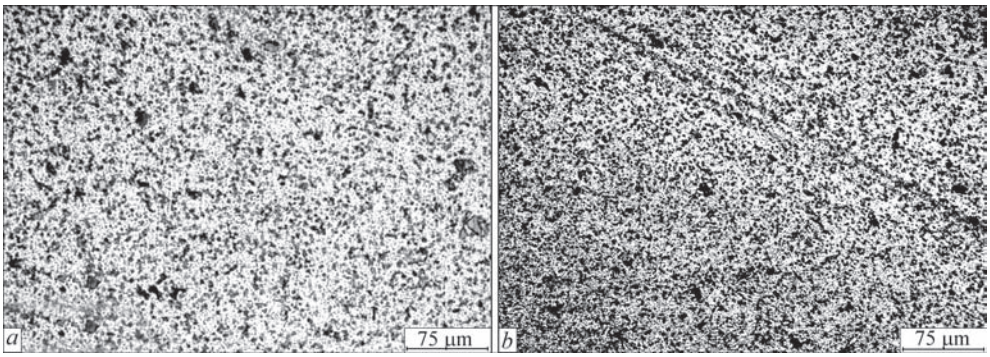


**Figure 6.** Microstructure of metal in weld nugget (*a*) and in TMIZ (*b*) of FSW joint

Investigation of the microstructure of welds showed that dynamic recrystallization of metal in the zone of intensive plastic deformation results in formation in the weld metal of a dispersed equilibrium structure with element size of 1–10 μm with individual intermetallics of 20–25 μm size, grouped into a conglomerate of grains of 70–150 μm size (Figure 6). Investigations of cyclic crack resistance revealed obvious differences in the diagram of the rate of fatigue macrocrack growth in the weld metal (Figure 7, curve *1*), for which after intensive bulk plastic shear deformation the mid-amplitude traditionally straight Paris section is transformed into the curvilinear section with the inflection point at $\Delta K = \Delta K_0 = 20$ MPa$\sqrt{\text{m}}$. This is characteristic exactly for the structure of the metal of weld, produced as a result of intensive plastic deformation of metal at FSW. Calculation of the size of cyclic plastic zone $r_p^c$ by the following formula:

$$r_p^c = 1/8\pi(\Delta K/\sigma_{0.2})^2, \quad (3)$$

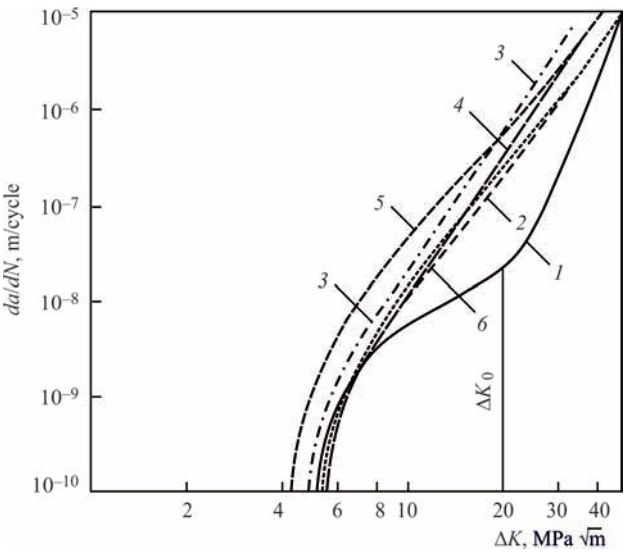


**Figure 7.** Diagrams of the rates of fatigue macrocrack growth in different zones of the joint produced by FSW: *1* — weld; *2* — TMIZ; *3* — HAZ; *4* — boundary of the zone of thermomechanical impact and heat-affected zone; *5* — base metal (samples cut across the rolling direction); *6* — base metal (samples cut out along the rolling direction)

where $\Delta K$ = 20 MPa$\sqrt{\text{m}}$, and yield limit $\sigma_{0.2}$ = = 340 MPa, gives value $r_p^c$ = 138 μm, that is in agreement with grain size (70–150 μm) of weld metal deformed during FSW. Thus, the inflection on the curve is indicative of the change of fracture mode, when at the tip of the fatigue macrocrack plastic deformation runs as multiplane dislocation slip in the volume of not one, but of several grains with involvement of grain-boundary processes. It can be also assumed that in such a deformed structure compressive residual stresses can arise [18], causing a considerable effect of crack tip closing. As a result, such weld metal, compared to base metal, demonstrates a higher fatigue threshold $\Delta K_{th}$ and cyclic fracture toughness $\Delta K_{fc}$ and, particularly, cyclic crack resistance index in mid-amplitude section of the diagram (Figure 7). Here, cyclic crack resistance of TMIZ and HAZ is somewhat lower, compared to weld metal: slightly in near-threshold section of the diagram and more in the mid- and high-amplitude sections (curves *2–4*). For instance, the fatigue macrocrack growth rate at medium $\Delta K$ ranges can be by an order of magnitude higher than this value for weld metal. HAZ metal has the lowest cyclic crack resistance among all the welded joint zones (curve *3*), although it is somewhat higher, compared to crack resistance of base metal, cut out across the rolling direction (curve *5*), particularly in near-threshold and mid-amplitude sections of the diagram. Here, crack resistance of TMIZ metal (curve *2*) is practically not inferior to crack resistance of base metal, cut out along the rolling direction (curve *6*). In the high-amplitude section of the diagram, crack resistance index (cyclic fracture toughness $\Delta K_{fc}$) of HAZ metal is much lower, compared to base metal, cut out across the rolling direction. Therefore, furtheron it is rational to study the possibility of its increase by changing the structural components of HAZ metal and its stress-strain state by postweld heat treatment of such joints [19].

Analysis of microfractographs of tested sample fractures is indicative of the fact that the micromechanism of fatigue crack growth in all the studied

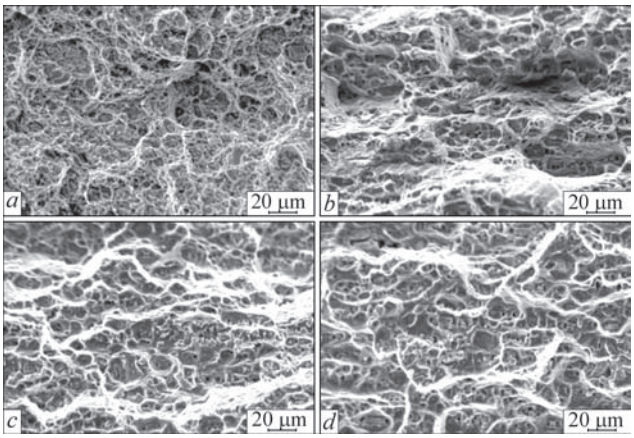


**Figure 8.** Microfractographs of fractures of samples failing in different joint zones: *a* — weld; *b* — TMIZ; *c* — boundary of the zones of thermomechanical impact and heat-affected zone; *d* — HAZ

zones of welded joints, produced by FSW, mainly is high-energy intensive pit one. Morphology of the pits and deformation ridges in weld metal fracture is the most finely-dispersed — individual fine cleavage sections (10–20 μm) are commensurate with weld structural elements (Figure 8, *a*). In TMIZ the number of sections of cleavage as a result of the impact of cyclic loads becomes greater, but they are divided by relatively large zones with deformation ridges (Figure 8, *b*), the most pronounced at the boundary of TMIZ and HAZ (Figure 8, *c*). Metal fracture morphology in the HAZ section is characterized by reduction of the number of extended deformation ridges and increase of the size of quasi-cleavage facets compared to weld metal (Figure 8, *d*), that, probably, is the reason for lowering of cyclic crack resistance index in this zone.

## Conclusions

1. The process of friction stir welding allows producing sound welded joints of D16T alloy with high values of static strength that is just by 4–5 % smaller than the respective values of base metal.

2. High values of strength of such joints are achieved due to lowering of the level of stress concentration in the points of weld to base metal transition, absence of defects (pores, oxide inclusions and hot solidification cracks), due to metal melting and solidification in the welding zone at GTAW, and formation of a fine-dispersed deformed structure of welds.

3. Owing to high indices of cyclic crack resistance of D16T alloy welded joints, produced by friction stir welding in the solid phase, their high structural strength is ensured that expands the possibilities for this alloy application in aerospace engineering.

1. Beletsky, V.M., Krivov, G.A. (2005) *Aluminium alloys (composition, properties, technology, application)*: Refer. Book. Ed. by I.N. Fridlyander. Kiev, Komintekh [in Russian].
2. Ishchenko, A.Ya., Labur, T.M., Bernadsky V.N., Makovetskaya, O.K. (2006) *Aluminium and its alloys in modern welded structures*. Kiev, Ekotekhnologiya [in Russian].
3. Ostash, O.P. (2015) *Fracture mechanics and strength of materials*: Refer. Book. Ed. by V.V. Panasyuk. Vol. 15: *Structure of materials and fatigue life of structural elements*. Lviv, SPOLOM [in Ukrainian].
4. Romaniv, O.N. (1979) *Fracture toughness of structural steels*. Moscow, Metallurgiya [in Russian].
5. Ostash, O.P., Gajvoronsky, O.A., Poznyakov, V.D., Kulyk, V.V. (2016) *Method of heat treatment of high-strength low-alloy carbon steels*. Pat. 105440, Ukraine. Publ. 25.03.2016 [in Ukrainian].
6. (1998) *Joint Aviation Requirements*, JAR 25.571.
7. Lozovskaya, A.V., Chajka, A.A., Bondarev, A.A. et al. (2001) Softening of high-strength aluminium alloys in different fusion welding processes. *The Paton Welding J*., **3**, 13–17.
8. Poklyatsky, A.G., Ishchenko, A.Ya., Grinyuk, A.A. et al. (2002) Non-consumable electrode argon-arc welding of aluminium alloys with arc oscillations. *Ibid*., **2**, 18–22.
9. Poklyatsky, A.G., Grinyuk, A.A. (2001) Effect of parameters of asymmetric and modulated currents on quality of aluminium alloy welded joints. *Ibid*., **7**, 33–36.
10. Poklyatsky, A.G. (2001) Peculiarities of formation of macroinclusions of oxide film in weld metal of aluminium alloys (Review). *Ibid*., **3**, 36–38.
11. Ishchenko, A.Ya., Lozovskaya, A.V., Sklabinskaya, I.E. (1999) Mechanism of retardation of solidification cracks in welding of aluminium alloys with scandium. *Avtomatich. Svarka*, **8**, 13–16 [in Russian].
12. Thomas, W.M., Nicholas, E.D., Needham, J.C. et al. *Friction stir butt welding*. Int. Pat. PCT/GB 92/02203; GB Pat. Appl. 9125978.8. Publ. 1991.
13. Pietras, A., Zadroga, L., Lomozik, M. (2004) Characteristics of welds formed by pressure welding incorporating stirring of the weld materials (FSW). *Welding International*, **1**, 5–10.
14. Shibayanagi, T. (2007) Microstructural aspects in friction stir welding. *J. of Japan Inst. of Light Metals*, **9**, 416–423.
15. Ishchenko, A.Ya., Poklyatsky, A.G. (2010) *Tool for friction stir welding of aluminium alloys*. Pat. 54096, Ukraine. Publ. 25.10.2010 [in Ukrainian].
16. Ostash, O., Uchanin, V., Semenets, J. et al. (2018) Evaluation of aluminium alloys degradation in aging aircraft. *Research Nondestructive Evaluation*, 29(**3**), 156–166.
17. *Standard test method for measurement of fatigue crack growth rates*. ASTM Standards, E647-93.
18. Bussu, G., Irving, P.E. (2003) The role of residual stress and heat affected zone properties on fatigue crack propagation in friction stir welded 2024-T351 aluminium joints. *Int. J. Fatigue*, **25**, 77–78.
19. Aydin, H., Bayram, A., Durgun, I. (2010) The effect of post-weld heat treatment on the mechanical properties of 2024-T4 friction stir-welded joints. *Mater. Des*., **31**, 2568–2577.

Received 26.10.2018